Alkane Separation

How to cite:
International Edition: doi.org/10.1002/anie.202300722
German Edition: doi.org/10.1002/ange.202300722

Metal-Organic Frameworks for C6 Alkane Separation

Feng Xie[+], *Liang Yu*[+], *Hao Wang*,* *and Jing Li**

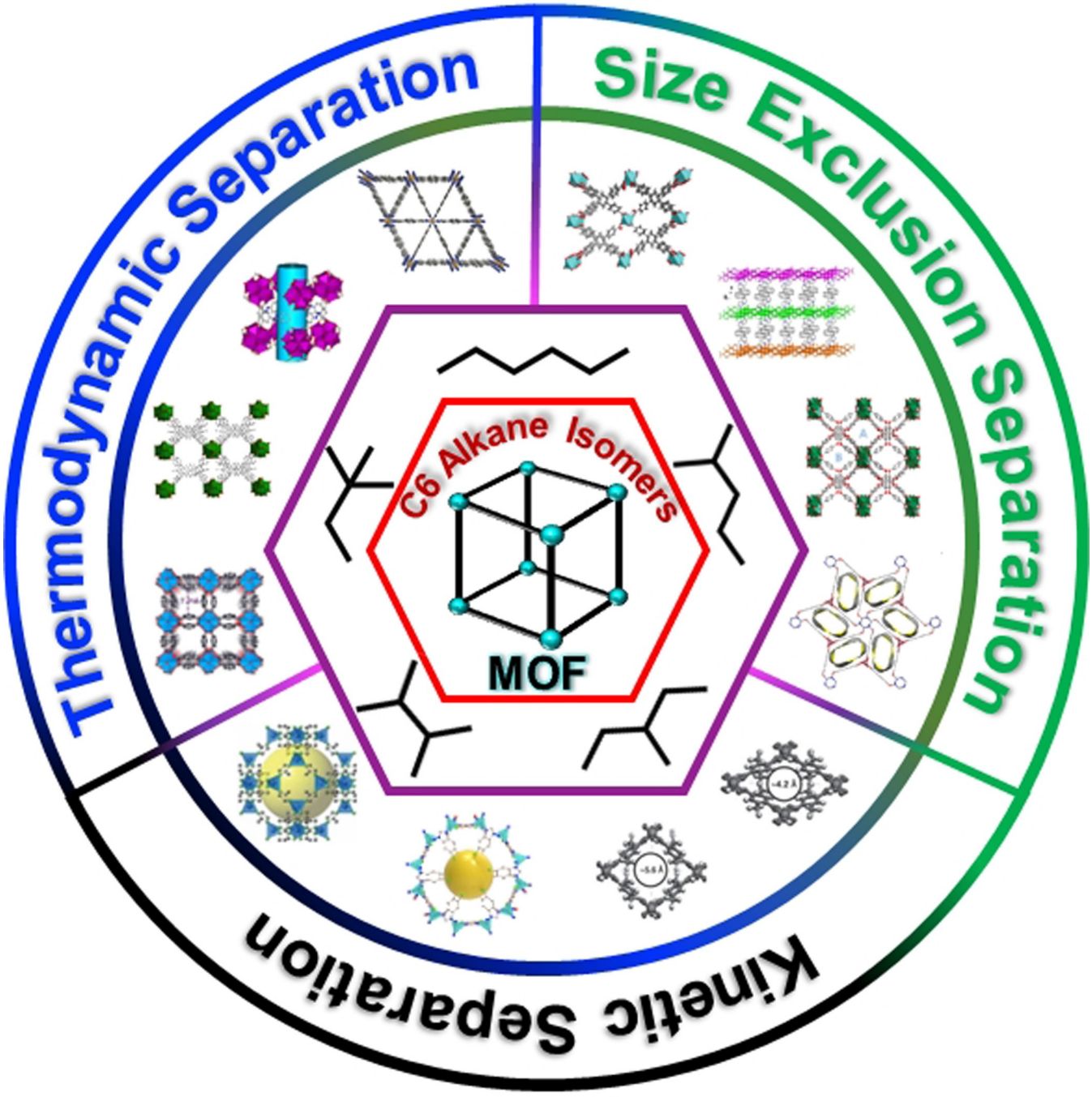

Abstract: The separation of alkane isomers is an important yet challenging process in the petrochemical industry. Being a crucial step to produce premium gasoline components as well as optimum ethylene feed, the current industrial separation by distillation is extremely energy intensive. Adsorptive separation based on zeolite is limited by insufficient adsorption capacity. Metal-organic frameworks (MOFs) hold enormous promise as alternative adsorbents due to their diverse structural tunability and exceptional porosity. Precise control of their pore geometry/dimensions has led to superior performance. In this minireview, we highlight the recent progresses in developing MOFs for the separation of C6 alkane isomers. Representative MOFs are reviewed based on their separation mechanisms. Emphasis is put on the material design rationale for achieving optimal separation capability. Finally, we briefly discuss the existing challenges, possible solutions, and future directions of this important field.

1. Introduction

The separation of C6 alkane isomers as a function of their branching, is a vital process in the petrochemical industry.[1] Upon catalytic isomerization reactions, linear and/or monobranched alkanes are to be used as olefin feed (for steam cracking production of ethylene and propylene) whereas more branched isomers possess higher octane numbers are to be used for premium gasoline blends.[2,3] Thus, the two groups of isomers need to be effectively separated for different end uses. In particular, efficient separation of monobranched and dibranched alkanes which may notably enrich the industrially deficient ethylene feed, is becoming increasingly important.

Currently, heat-driven distillation is the dominant method for C6 alkane isomers separation, but it suffers from massive energy consumption and high installation cost.[4,5] As an alternative or supplementary technology to distillations, adsorptive separation using porous adsorbents is potentially more energy efficient and cost effective.[6,7] However, owing to their chemical inertness and similar physicochemical properties, adsorptive separation of C6 alkane isomers is challenging as the only parameters that can be considered are their molecular shape and dimension which are also quite similar.[8,9] As such, efficient discrimination of these isomers has stringent requirements on the pore shape/aperture of the adsorbents in order to precisely match the shape and kinetic diameter of the adsorbates. As a benchmark adsorbent for alkane separation, zeolite 5 A featuring a pore aperture of 5 Å has the ability to fully separate linear alkanes from their branched isomers.[10–12] However, the relatively low adsorption capacity limits its separation efficiency. Moreover, it is incapable of separating monobranched and dibranched alkanes, restricting its wider applicability. On the other hand, ZSM-5 with 1D channels of 5.5 Å diameter can discriminate monobranched and dibranched alkane isomers, but again, with severely limited adsorption capacity.[13,14]

Metal-organic frameworks (MOFs) as a newer family of porous adsorbents are particularly desirable in addressing industrially challenging separations of hydrocarbons because of their diverse structural modularity, exceptional porosity, highly tunable pore size, pore shape, and surface functionality.[15–18] These unique features of MOFs have led to their excellent performance for the separation of physically and chemically similar mixtures including olefin/paraffin,[19–23] alkyne/olefin,[24,25] carbon dioxide/acetylene,[26–28] and alkane isomers.[29,30] In particular, the successful practice of reticular chemistry has enabled the precise control of pore structures of MOFs, affording adsorbents with desired discrimination capability toward C6 alkane isomers with different degrees of branching (Table 1). In 2013, Long et al. reported a proof-of-concept study of thermodynamic separation of hexane isomers according to the different adsorption affinity.[31] Since then, the major research efforts have been devoted to the design of novel MOFs and the optimization of their pore structures for high-efficiency separation of C6 alkane isomers (Scheme 1). In general, the separation mechanisms can be classified into three categories, thermodynamically driven, kinetically driven, and selective molecular exclusion processes. Over the past few years, a number of MOFs with tailored pore structures have succeeded in full separation of alkane isomers, especially the splitting of monobranched and dibranched alkanes. Thus, it is of a timely necessity to provide a broader insight into the design of MOF adsorbents and their potential applicability for alkane isomers separation.

In this minireview, we summarize recent development of microporous MOFs for the separation of C6 alkanes, including early examples based on thermodynamically driven routes, as well as the latest tailor-made structures following highly efficient size exclusion processes (Table 2). We discuss the progresses made so far on the three separation mechanisms mentioned above. Under each category, structures and separation performance of representative MOFs are presented, with a focus particularly on the material design and structure/pore tuning strategies. Lastly, we also lay out existing challenges and possible solutions, as well as an outlook of future directions.

[*] F. Xie,[+] Prof. Dr. J. Li
Department of Chemistry and Chemical Biology, Rutgers University
Piscataway, NJ 08854 (USA)
E-mail: jingli@rutgers.edu

L. Yu,[+] Prof. Dr. H. Wang, Prof. Dr. J. Li
Hoffmann Institute of Advanced Materials, Shenzhen Polytechnic
7098 Liuxian Boulevard, Shenzhen, Guangdong 518055 (P. R. China)
E-mail: wanghao@szpt.edu.cn

[+] These authors contributed equally to this work.

Table 1: Physicochemical properties of C6 alkane isomers, including boiling point, kinetic diameter, and research octane number.[9,46]

Alkane Molecule	Structural Formula	Boiling Point [K]	Kinetic Diameter [Å]	Research Octane Number
n-hexane	$CH_3(CH_2)_4CH_3$	341.6–342.2	4.5	24.8
2-methylpentane	$CH_3CH(CH_3)(CH_2)_2CH_3$	333–335	5.0–5.5	73.4
3-methylpentane	$CH_3CH_2CH(CH_3)CH_2CH_3$	336.0–336.8	5.0–5.5	74.5
2,2-dimethylbutane	$CH_3C(CH_3)_2CH_2CH_3$	322.8–323	6.2	91.8
2,3-dimethylbutane	$CH_3CH(CH_3)CH(CH_3)CH_3$	331.0–331.4	5.6	101.7

2. Thermodynamic Separation of C6 Alkane Isomers

Thermodynamic separation is based on the different interaction strength between the adsorbent pore surface and the gas/vapor molecules.[16] When the pore apertures of adsorbents are large enough to allow guest molecules to pass through freely, some are preferentially adsorbed on the adsorbent surface over others, depending on the surface chemistry of adsorbents and the physicochemical properties of the guest molecules including size/shape, polarizability, dipole moment, and quadrupole moment.[53] For example, some specific functional sites, including open metal sites,[54] hydrogen bonding sites,[26] and other polar groups,[55,56] can be selectively introduced into the internal pores of the adsorbents to dramatically enhance the binding strength between adsorbents and specified guest molecules to achieve desirable separation performance. For gas adsorption in the interior of porous materials, the interaction potential energy of the process is the sum of the adsorbate-adsorbent interaction potentials. For gas/vapor mixtures of high similarity, their adsorptive separation relies on the difference of their interaction potentials with the pore surface, while these potentials are accumulative.

The first example of using microporous MOF to separate alkane isomers was reported by Chen et al. in 2006.[47] They successfully separated C6 alkanes employing gas chromatography with MOF-508 as the column filler. In 2013, Herm et al. reported a microporous framework $Fe_2(BDP)_3$ (BDP = 1,4-benzenedipyrazolate) featuring triangular channels which shows efficient discrimination of hexane isomers with different shapes.[31] The pore width of the 1D channels of $Fe_2(BDP)_3$ is large enough to readily accommodate all hexane isomers (Figure 1a–1c) and thus the separation is mainly directed by a thermodynamic mechanism. Single-component adsorption isotherms and isosteric heats of adsorption of these isomers suggest that the lower degree of branching would contribute to the stronger adsorption strength (Figure 1d–1h). In breakthrough experiments conducted with an equimolar mixture of n-hexane (nHEX), 2-methylpentane (2MP), 3-methylpentane (3MP), 2,3-dimethylbutane (23DMB), and 2,2-dimethylbutane (22DMB), dibranched isomers eluted first, followed by monobranched isomers, and finally the linear hexane in the sequence of

Feng Xie received his B.S. degree from Jilin University, China and M.S. degree in Chemistry from King Abdullah University of Science and Technology, Saudi Arabia, in 2019 under the guidance of Professor Yu Han. He is currently a doctoral student in Professor Jing Li's research group at Rutgers University, United States. His research focuses mainly on the design and optimization of functional porous materials for energy-related applications, with an emphasis on adsorption-based molecular separations.

Liang Yu was a research assistant in the Hoffmann Institute of Advanced Materials (HIAM) at Shenzhen Polytechnic from 2018 to 2020. He is currently a third-year doctoral student in the School of Chemistry and Chemical Engineering of South China University of Technology. His research focuses on the design and preparation of novel metal–organic frameworks and their applications in gas separation.

Hao Wang received his B.S. degree from Wuhan University, China, in 2012, and Ph.D. degree from Rutgers University, United States, in 2018. He then joined the Hoffmann Institute of Advanced Materials (HIAM) at Shenzhen Polytechnic, where he is currently an Associate Professor. His research focuses on the design of novel crystalline porous materials and their applications in industrially relevant separations.

Jing Li received her Ph.D. degree from Cornell University in 1990 under the guidance of Professor Roald Hoffmann. She joined the chemistry faculty at Rutgers University in 1991 as an Assistant Professor. She was promoted to Associate Professor in 1996, to Full Professor in 1999, and to Distinguished Professor in 2006. Her research centers on the development of functional materials (including MOFs and hybrid semiconductors) and their potential applications in renewable, sustainable, and clean energy technologies.

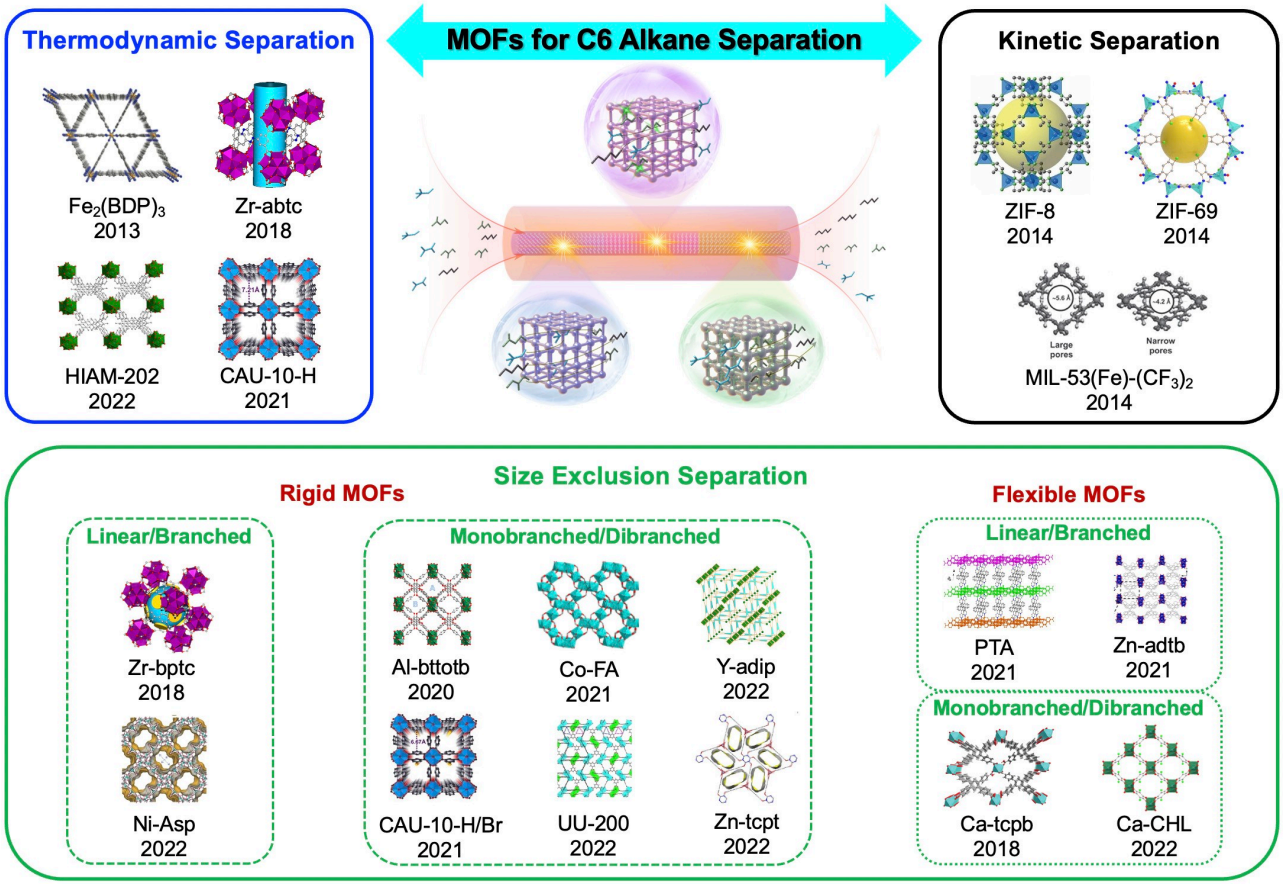

Scheme 1. Schematic representation of C6 alkane isomers separation by MOFs following the three separation mechanisms and representative structures reported with high separation performance. $Fe_2(BDP)_3$: reproduced with permission.[31] Copyright 2013, AAAS. Zr-abtc & Zr-bptc: reproduced with permission.[30] Copyright 2018, Springer Nature. HIAM-202: reproduced with permission.[32] Copyright 2022, American Chemical Society. CAU-10-H/Br: reproduced with permission.[33] Copyright 2021, Elsevier. ZIF-8 & ZIF-69: reproduced with permission.[34,35] Copyright 2014, AAAS. MIL-53(Fe)-$(CF_3)_2$: reproduced with permission.[36] Copyright 2014, Wiley-VCH. Ni-Asp: reproduced with permission.[37] Copyright 2022, American Chemical Society. Al-bttotb: reproduced with permission.[38] Copyright 2020, American Chemical Society. Co-FA: reproduced with permission.[39] Copyright 2021, Wiley-VCH. Y-adip: reproduced with permission.[40] Copyright 2022, American Chemical Society. UU-200: reproduced with permission.[41] Copyright 2022, Wiley-VCH. Zn-tcpt: reproduced with permission.[42] Copyright 2022, Wiley-VCH. PTA: reproduced with permission.[43] Copyright 2021, Wiley-VCH. Zn-adtb: reproduced with permission.[44] Copyright 2021, American Chemical Society. Ca-tcpb: reproduced with permission.[29] Copyright 2018, Royal Society of Chemistry. Ca-CHL: reproduced with permission.[45] Copyright 2022, Wiley-VCH.

22DMB > 23DMB > 3MP > 2MP > nHEX (Figure 1i). Moreover, configurational-bias Monte Carlo simulations indicated that the number of carbon atoms that can interact with the pore surface of $Fe_2(BDP)_3$ reduces with the increasing degree of branching. Dibranched isomers have the weakest interactions with MOF pore surface, resulting in the shortest retention in the column. Further experimental evaluation demonstrated that the separation efficiency of $Fe_2(BDP)_3$ is superior to the commercial standard compared with benchmark zeolites.

Based on the deliberately selected isophthalete-based tetratopic ligand with appropriate dimensions, Wang et al. developed a Zr-MOF with 8-connected hexanuclear Zr_6 secondary building units and 4-connected tetracarboxylates ligand, Zr-abtc ($Zr_6O_4(OH)_8(H_2O)_4(abtc)_2$, abtc = 3,3′,5,5-′azobenzenetetracarboxylate).[30] Zr-abtc features a scu-type structure with 1D channels of 7 Å diameter (Figure 2a). As expected, it accommodates all C6 alkane isomers but thermodynamically favors nHEX because of its stronger interactions with the 1D channels (Figure 2b–2d), which is similar to $Fe_2(BDP)_3$. The results from single component adsorption and multicomponent breakthrough (Figure 2e) experiments indicate that Zr-abtc is capable of thermodynamically driven separation of all three C6 isomers with a high mono/dibranched separation factor.

3. Kinetic Separation of C6 Alkane Isomers

Kinetic separation is based on the difference in the diffusion rates of guest molecules in the pores of adsorbents.[53] For the separation process achieved through kinetic effect, pore size of the adsorbent is the key factor which determines the adsorption selectivity and separation efficiency. In this case, the dimension of the pore aperture is typically close to the kinetic diameter of the component to be separated. Gas/

Table 2: Representative MOFs for adsorptive separation of C6 alkane isomers.

MOF	Surface Area [$m^2 g^{-1}$]	Pore Aperture [Å]	Alkane Isomers (uptake, $mmol g^{-1}$)	T [°C]	Separation Mechanism	Ref.
MOF-508	946	≈4.0	nHEX; 2MP; 22DMB	–	Chromatography	[47]
$Fe_2(bdp)_3$	1230	≈4.9	nHEX(1.32); 2MP(1.18); 3MP(1.27); 23DMB(1.37); 22DMB(1.22)	160	Thermodynamic	[31]
Zr-abtc	1318	≈4.5	nHEX(1.28); 3MP(1.02); 23DMB(0.58)	150	Thermodynamic	[48]
MIL-101 (Cr)	3990	10–20	nHEX(10.2); 2MP(9.2); 22DMB(8.6)	40	Thermodynamic	[49]
ZIF-76	1560	≈5	nHEX; 3MP; 22DMB	125	Thermodynamic	[11]
CAU-10-H	483	6.2	nHEX(1.56); 3MP(1.1); 22DMB(0.63)	30	Thermodynamic	[33]
HIAM-202	543	6–7	nHEX(4.35); 3MP(4.26); 22DMB(1.57)	30	Thermodynamic	[32]
ZIF-8	1810	≈3.4	nHEX; 3MP; 22DMB	125	Kinetic	[11]
MIL-53(Fe)-$(CF_3)_2$	–	4.2/5.6	nHEX(0.37); 3MP(0.35); 22DMB(0.31)	40	Kinetic	[36]
ZIF-8	–	–	nHEX(1.58); 2MP(0.32); 3MP(0.20); 23DMB(0.05); 22DMB(0.02)	100	Kinetic	[50]
			nHEX(0.86); 2MP(0.25); 3MP(0.15); 23DMB(0.04); 22DMB(0.02)	150		
			nHEX(0.36); 2MP(0.17); 3MP (0.1); 23DMB(0.03); 22DMB(0)	200		
ZIF-8	1285	≈3.4	nHEX(5.9); 2MP(1.05)	25	Kinetic	[35]
ZIF-69	845	7.8	nHEX(3.95); 2MP(1.16)	25	Kinetic	[35]
$Fe_3(\mu_3\text{-}O)(6fdca)_3$	270	8/12	nHEX(0.79); 3MP(0.58); 23DMB(0.43)	25	Kinetic	[51]
$Zn_2(Hbdc)_2(dmtrz)_2$	552	6.7	nHEX (1.53); 3MP (1.40); 22DMB (0.40)	25	Kinetic	[52]
Zr-bptc	1030	≈4.5	nHEX(1.51); 3MP(0.29); 23DMB(0)	150	Size exclusion	[48]
Zn-adtb	273	6.5	nHEX(1.4); 3MP(0.23); 23DMB(0.05)	30	Size exclusion	[44]
Ni-asp	217	5.9	nHEX(1.49); 3MP(0.2); 22DMB(0.16)	30	Size exclusion	[37]
Al-bttotb	572	5.6	nHEX(1.76); 3MP(1.1); 23DMB(0.1)	30	Size exclusion	[38]
Zn-tcpt	1135	≈4.9	nHEX(3.26); 3MP(2.14); 22DMB(0.08)	30	Size exclusion	[42]
UU-200	482	≈5	nHEX(1.7); 3MP(1.14); 22DMB(0.09)	30	Size exclusion	[41]
CAU-10-H/Br	463	5.5	nHEX(1.46); 3MP(0.7); 22DMB(0.09)	30	Size exclusion	[33]
HIAM-302	388	–	nHEX(1.92); 3MP(1.1); 22DMB(0.16)	25	Size exclusion	[40]
Co-fa	365	5.5	nHEX(1.5); 2MP(1.6); 3MP(1.6); 23DMB(0.28); 22DMB(0.22)	30	Size exclusion	[39]
PTA	–	≈5.7	nHEX(2.1); 3MP(1.74)	30	Size exclusion	[43]
			nHEX(2.05); 3MP(0.1)	50		
HIAM-203	499	≈4.8	nHEX(1.7); 3MP(1.43); 22DMB(0.07)	30	Size exclusion	[45]
			nHEX(0.95); 3MP(0.02); 22DMB(0)	150		
Ca-tcpb	220	≈5.5	nHEX(1.62); 3MP(1.54); 22DMB(0.10)	60	Size exclusion	[29]
			nHEX(1.14); 3MP(0.12); 22DMB(0)	120		

Abbreviations: bdp = 1,4-benzenedipyrazolate; abtc = 3,3′,5,5′-azobenzenetetracarboxylate; 6fdca = 2,2-bis(4-carboxyphenyl)-hexafluoropropane; dmtrz = 3,5-dimethyl-1H,1,2,4-triazole; bptc = 3,3′,5,5′-biphenyltetracarboxylate; adtb = 4,4′,4″,4‴-(anthracene-9,10-diylidenebis-(methanediylylidene))tetrabenzoic acid; asp = L-aspartic acid; bttotb = 4,4′,4″-(benzene-1,3,5-triyltris(oxy))tribenzoic acid; tcpt = 2,4,6-tris(4-carboypheneoxy)-1,3,5-triazine; fa = formate; tcpb = 1,2,4,5tetrakis(4carboxyphenyl)benzene.

vapor molecules with higher diffusion mobility can favorably enter the pore and occupy the pore space preferentially over other competing components, thereby achieving a good separation performance. This non-equilibrium separation may not be reflected in the adsorption amounts but is notable through adsorption rate evaluation and multicomponent column breakthrough tests.[57]

One of the prototype and representative examples of MOFs capable of kinetic separation is ZIF-8 (ZIF: zeolitic imidazolate framework), which represents a state-of-the-art MOF with high stability, facile synthesis, and structural flexibility. It exhibits unique adsorption behavior toward gas/vapor molecules, including alkane isomers.[11,35,58] ZIF-8 is one of the most extensively studied MOFs. It crystallizes in sodalite structure with cage like pores (Figure 3a).[59] The large cages (≈11.4 Å) are connected through smaller pore windows (made of six-membered rings) with an aperture of ≈3.4 Å. ZIF-8 possesses high surface area (≈1810 $m^2 g^{-1}$) and pore volume (≈0.66 $cm^3 g^{-1}$). Chang et al. observed that ZIF-8-coated capillary columns are highly capable of separating branched alkanes from their linear isomers by gas chromatography.[60] The chromatograms show that ZIF-8 nanocrystal coated capillaries offer excellent features for high-resolution gas chromatographic separation of linear alkanes due to their smaller molecular dimensions and strong van der Waals interaction between linear alkanes and the hydrophobic inner pore surfaces.

In a follow-up study, Henrique et al. investigated the adsorption and separation of C6 alkane isomers on ZIF-8 through fixed bed adsorption experiments.[50] The sorption dynamics of C6 alkane isomers on ZIF-8 were evaluated by a series equilibrated adsorption isotherms at various temperatures (Figure 3b–3f). The results show the following trend of adsorption: nHEX > 2MP > 3MP > 23DMB > 22DMB. In addition, the adsorption selectivity, defined as the ratio of the total adsorbed amount of linear and monobranched

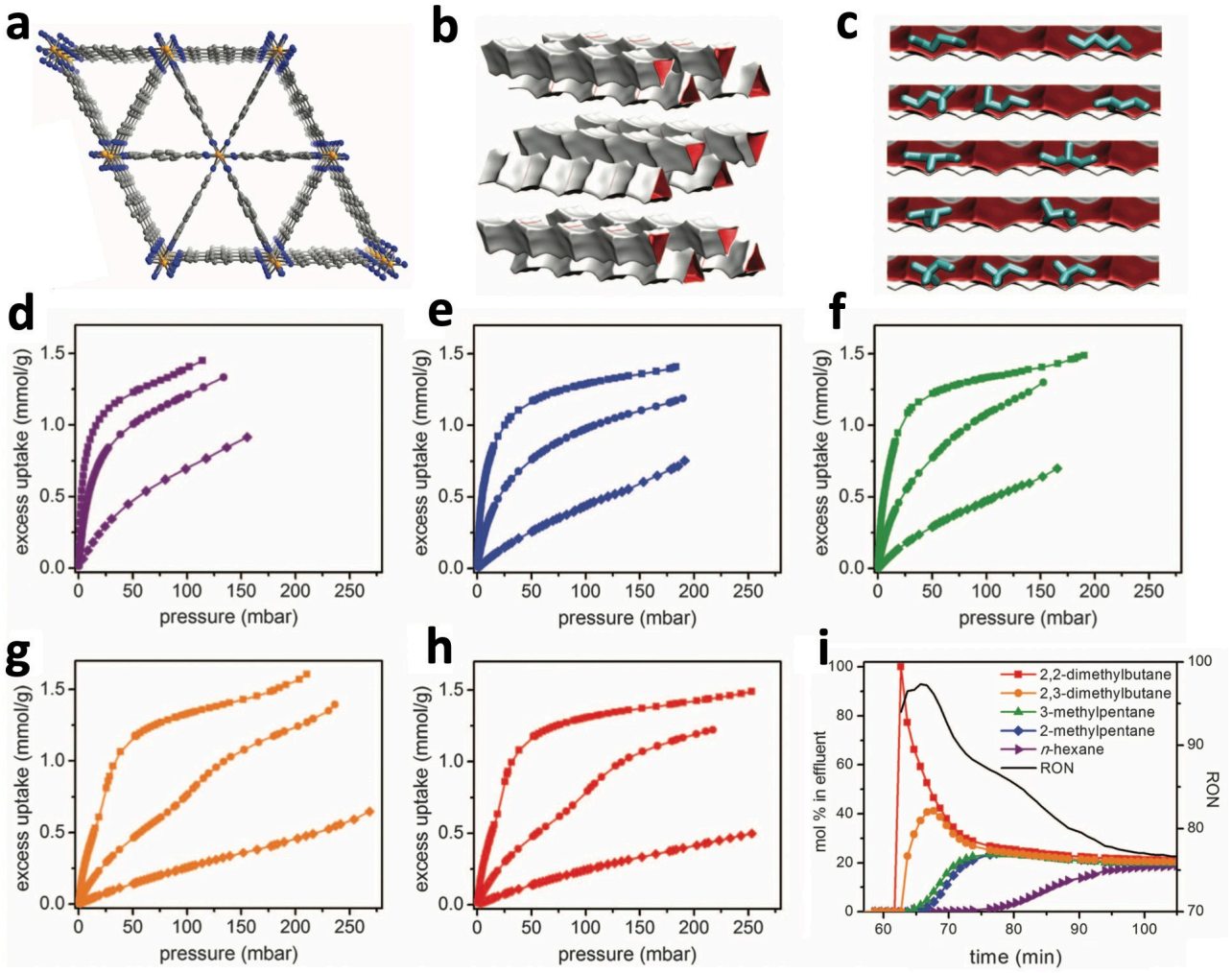

Figure 1. (a) Crystal structure of $Fe_2(BDP)_3$. (b) The van der Waals surfaces associated with the corrugated triangular channels. (c) Snapshots of the C6 alkane isomers within the channels of $Fe_2(BDP)_3$ at 160 °C as observed in Configurational-bias Monte Carl simulations. (d–h) Single-component adsorption isotherms for nHEX (d), 2MP (e), 3MP (f), 23DMB (g), and 22DMB (h) in $Fe_2(BDP)_3$ at 130 °C (square), 160 °C (circle), and 200 °C (diamond). (i) Experimental quinary breakthrough curves of equimolar C6 alkane isomers for a $Fe_2(BDP)_3$ packed bed at 160 °C. Reproduced with permission.[31] Copyright 2013, American Association for the Advancement of Science.

isomers and the total adsorbed amount of dibranched isomers, ranges between 34 and 55 (at total pressure of 0.5–0.1 bar) which is considered very high. The separation performance of C6 alkane isomers by ZIF-8 was further evaluated through multicomponent breakthrough experiments on an equimolar mixture (Figure 3g–3i). The results from adsorption isotherms and characteristic diffusivities calculations suggest that the separation of nHEX is equilibrium based in contrast with the separation of branched isomers which is kinetically controlled. The diffusivity of monobranched alkane isomers in ZIF-8 is two orders of magnitude lower than that of the linear nHEX, and the diffusivity of dibranched alkanes is three times lower than those of the mono-branched ones. These results demonstrate ZIF-8 is capable of separating the linear nHEX from its branched isomers and partially discriminating the mono-branched and dibranched isomers via kinetic mechanism.

By functionalizing the organic constitutive moieties of MOFs to modulate the adsorption properties, Mendes et al. reported a flexible and perfluoro functionalized Fe-MOF made of dicarboxylate, MIL-53(Fe)-$(CF_3)_2$, for the kinetically controlled separation of C6 alkane isomers.[36] The bulky perfluoro -CF_3 groups on the terephthalate ligand of the MIL-53(Fe) strongly affect the accessibility of the pores and the diffusivity of different alkane isomers. MIL-53(Fe)-$(CF_3)_2$ has 1D channels that can transform between its large-pore (LP) and narrow-pore (NP) states, with pore apertures of 5.6 Å and of 4.2 Å, respectively, as a result of its dynamic structural change (Figure 4a).[61] The adsorption isotherms revealed that the compound can accommodate all three C6 isomers including nHEX, 3MP, and 22DMB with similar adsorption capacities (Figure 4b). However, the calculated adsorption kinetics show obvious differences in diffusivity between the dibranched isomer and the 3MP/nHEX molecules (Figure 4c). In the multicomponent column breakthrough experiments, nHEX exhibited noticeable retention followed by 3MP, while the dibranched 22DMB eluted immediately out from the column at the beginning of the

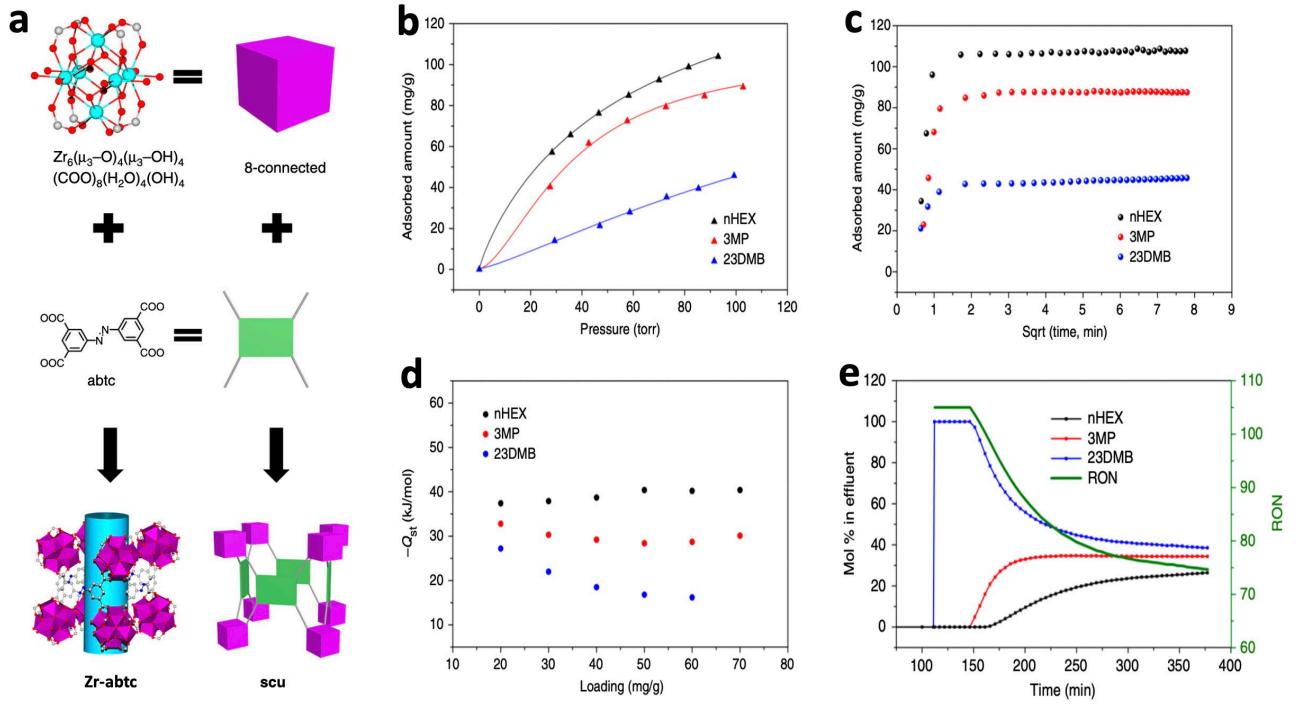

Figure 2. (a) Secondary building unit, organic ligand, crystal structure, and topology of Zr-abtc. (b) Adsorption isotherms of nHEX, 3MP, and 23DMB at 150 °C on Zr-abtc. (c) Adsorption rates (at 100 torrs) of nHEX, 3MP, and 23DMB at 150 °C on Zr-abtc. (d) The heats of adsorption for C6 alkane isomers on Zr-abtc. (e) Experimental ternary breakthrough curves of an equimolar mixture of C6 alkane isomers collected from a Zr-abtc packed bed at 150 °C. Reproduced with permission.[30] Copyright 2018, Springer Nature.

measurement. This work illustrates a kinetically controlled molecular separation of the dibranched isomer from lower branched hexane isomers (Figure 4d).

4. Size-Exclusion Based Separation of C6 Alkane Isomers

Separation based on selective size exclusion refers to the sieving of the molecules to be separated making use of the differences in their size/shape as well as the pore structure of the adsorbents. In such a separation process, certain components in a gas/vapor mixture will be prevented from entering the pores of the adsorbent, while other components can smoothly enter the pores and be adsorbed. Selective size exclusion is considered as the ideal separation scenario because of its infinite adsorption selectivity.[4] Compared with conventional porous materials, MOFs have huge advantages in rational design and fine-tuning of the pore shape and pore aperture,[62] which is crucial for achieving size exclusion separation with optimal separation capacity.

4.1. Size-Exclusion Based Separation of Linear and Branched Alkanes

Despite the considerable potential of above-mentioned MOFs for the separation of C6 alkane isomers, they still suffer from relatively low selectivity for real-world applications. The pore aperture of a MOF, which is essential to achieve high-efficiency splitting of alkane isomers, is commonly determined by the dimension of the organic ligand. Thus, one can finely tune the pore size of a MOF through ligand design guided by reticular chemistry. Applying topology-directed MOF design strategy (or reticular chemistry), Wang et al. synthesized three Zrbased MOFs using deliberately selected isophthalate based tetratopic organic linkers with appropriate molecular dimensions (Figure 5a), and the pore shape and pore size of the MOFs were systematically adjusted.[30] A ftw-type MOF, Zr-bptc ($Zr_6O_4(OH)_4(bptc)_3$, bptc = 3,3′,5,5′-biphenyltetracarboxylate) with optimized pore structure was achieved, which exhibits an exceptionally high selectivity and adsorption capacity for the separation of C6 alkane isomers. Zr-bptc features a very robust structure and high porosity with a BET surface area of 1030 $m^2 g^{-1}$. It possesses cage-like large pores connected through narrow pore aperture of ≈4.5 Å. Behaving similarly to zeolite 5 A, it adsorbs linear alkanes but excludes branched isomers (Figure 5b–5c). Notably, it has an adsorption capacity of ≈13 wt% of nHEX at 150 °C, significantly higher than that of zeolite 5 A under identical conditions (≈8 wt%) (Figure 5d). This could be attributed to its noticeably higher surface area compared to that of zeolite 5 A. Its separation of nHEX based on selective size exclusion was confirmed by both adsorption isotherms and multicomponent column breakthrough measurements which demonstrated substantial retention of nHEX while branched

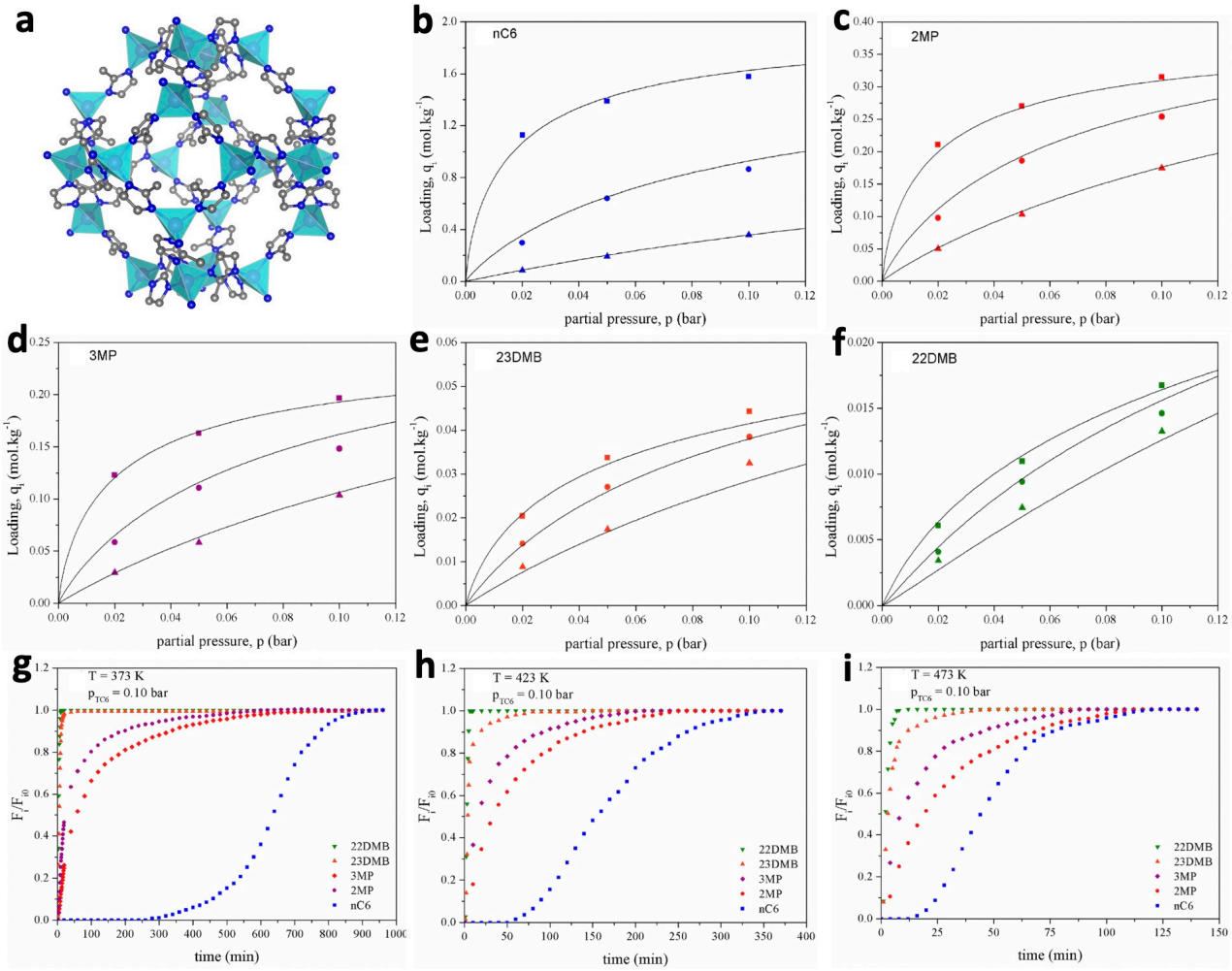

Figure 3. (a) The ZIF-8 structure. (b–f) Adsorption isotherms of nHEX (b), 2MP (c), 3MP (d), 23DMB (e), and 22DMB (f) on ZIF-8 at 373 K (square), 423 K (circle), and 473 K (triangle). (g–i) Experimental quinary breakthrough curves of equimolar C6 alkane isomers for a ZIF-8 packed bed at 373 K (g), 423 K (h), and 473 K (i). (b–i) are reproduced with permission.[50] Copyright 2019, American Chemical Society.

isomers eluted immediately out of the column with essentially no notable retention (Figure 5e).

4.2. Size-Exclusion Based Separation of Monobranched and Dibranched Alkanes

As stated in the previous section, compared to the splitting of linear and monobranched alkanes that can be accomplished by zeolite 5 A, full separation of monobranched and dibranched is more important and much needed in petrochemical industry. Recently, Yu et al. reported a robust Al-based MOF (Al-bttotb, bttotb = 4,4′,4″-(benzene-1,3,5-triyltris(oxy))tribenzoicacid) exhibiting strong sieving effect for the separation of linear/monobranched and dibranched alkanes.[38] Al-bttotb is constructed from 1D chain of corner-sharing AlO_6 polyhedra and bttotb, forming a three-dimensional (3D) network consisting two types of 1D channels with a square-shaped cross section (Figure 6a). It has a BET surface area of 572 $m^2 g^{-1}$ and a uniform pore size of 5.6 Å, which is comparable to the kinetic diameter of monobranched alkanes. It adsorbs a large amount of nHEX and 3MP (151 and 94 $mg g^{-1}$, respectively) while almost completely excluding 22DMB at room temperature (Figure 6b). In addition, the dynamic adsorption experiments showed that Al-bttotb adsorbs nHEX and 3MP with relatively high adsorption kinetics (Figure 6c). Single crystal X-ray diffraction analysis of adsorbate-loaded Al-bttotb coupled with theoretical calculations revealed that both nHEX and 3MP molecules are preferentially adsorbed in channel B in pairs while the larger 22DMB (6.2 Å) was excluded by the MOF channels. Multicomponent column breakthrough measurements further confirmed the complete separation of the monobranched and dibranched alkane isomers (Figure 6d). In a more recent study, Gong et al. carried out a comprehensive study of adsorption and separation of alkanes by a series of representative adsorbents including zeolite 5A, ZSM-5, Zr-abtc, Co-FA, and Al-bttotb.[63] Through single-component adsorption, multicomponent column breakthrough measurements, and more importantly, fixed bed

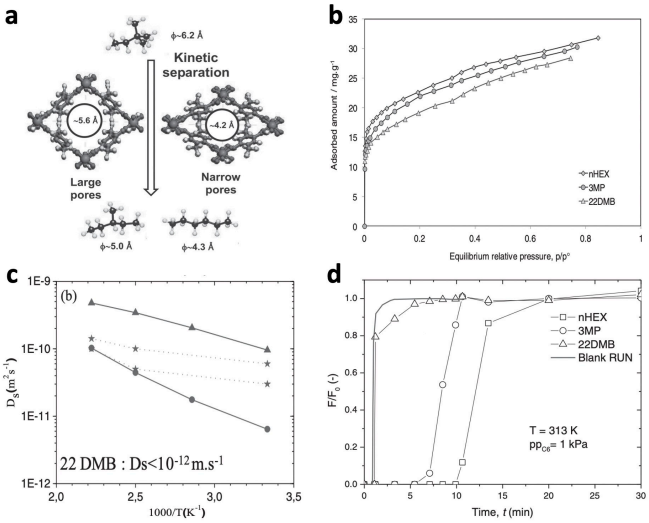

Figure 4. (a) Illustration of the 1D channels of MIL-53(Fe)-$(CF_3)_2$ at two different states (LP and NP) and their corresponding pore sizes. (b) Adsorption isotherms of nHEX, 3MP, and 22DMB in MIL-53(Fe)-$(CF_3)_2$ at 313 K. (c) Self-diffusion coefficients of nHEX (solid triangles) and 3MP (solid circles) as a function of 1000/T in MIL-53(Fe)-$(CF_3)_2$. The diffusion coefficient of 22DMB is below 10^{-12} m s^{-1}. (d) Experimental ternary breakthrough curves of equimolar C6 alkane isomers for a MIL- 53(Fe)-$(CF_3)_2$ packed bed at 313 K. Reproduced with permission.[36] Copyright 2014, Wiley-VCH.

separation of 180-component full range of naphtha, the authors demonstrated that adsorbents that can fully split monobranched and dibranched alkanes are superior for the real-world separation processes. In particular, Al-bttotb exhibits excellent separation efficiency for naphtha separation with high removal rate for monobranched alkanes, producing eluents with high RON.

Although suitable pore dimensions endow MOF adsorbents with the capability of selective molecular exclusion, they generally suffer from relatively low porosity which leads to their limited adsorption capacity. In attempt to seek adsorbents that feature both optimal pore dimensions and high porosity so as to break the trade-off between adsorption capacity and selectivity, Yu et al. reported the design and synthesis of Zn-tcpt (tcpt = 2,4,6-tris(4-carboxyphenoxy)-1,3,5-triazine), a MOF with high surface area but a small pore aperture (Figure 7a).[42] Zn-tcpt features a two-fold interpenetrated structure of hms nets, with a BET surface area of 1135 $m^2 g^{-1}$ and a uniform pore size of ≈4.9 Å (Figure 7b). It takes up substantial amount of nHEX and 3MP with uptakes of 280 and 184 mg g^{-1}, respectively, but fully excludes the dibranched 22DMB. The uptake values of Zn-tcpt are notably higher than those of the previously reported adsorbents that can split monobranched and di-branched alkanes (Figure 7c). The excellent separation capability of Zn-tcpt was evidenced by the experimental ternary breakthrough results, showing that Zn-tcpt can separate the C6 alkane isomers into individual components with high performance (Figure 7d). The di-

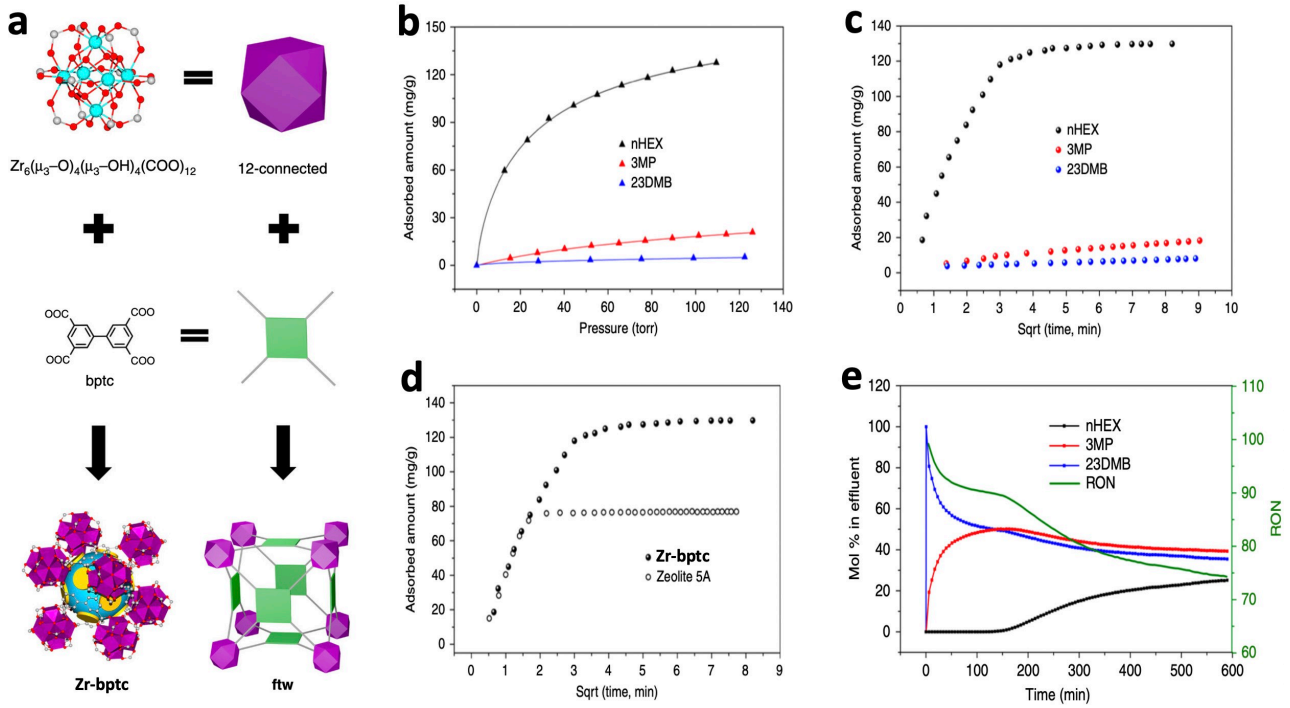

Figure 5. (a) Secondary building unit, organic ligand, crystal structure, and topology of Zr-bptc. (b) Adsorption isotherms of nHEX, 3MP, and 23DMB at 150 °C on Zr-bptc. (c) Adsorption rates (at 100 torrs) of nHEX, 3MP, and 23DMB at 150 °C on Zr-bptc. (d) nHEX adsorption rates of Zr-bptc and benchmark zeolite 5 A at 150 °C and 100 torrs. (e) Experimental ternary breakthrough curves of equimolar C6 alkane isomers for a Zr-bptc packed bed at 150°C. Reproduced with permission.[30] Copyright 2018, Springer Nature.

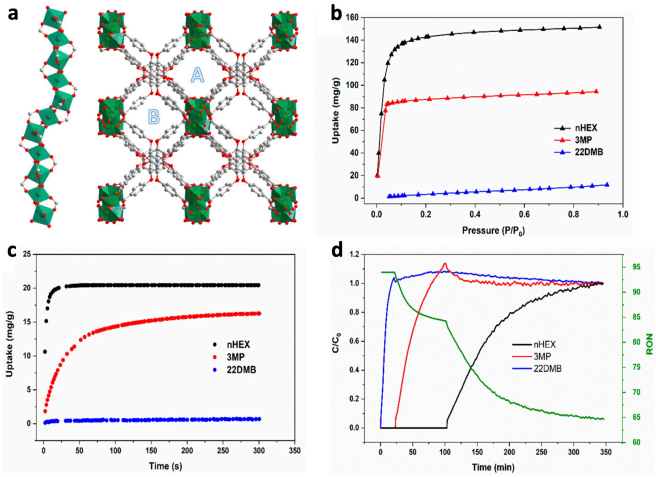

Figure 6. (a) Array of corner-sharing AlO_6 polyhedra and crystal structure of Al-bttotb showing two types of channels. (b) Adsorption isotherms of nHEX, 3MP, and 22DMB on Al-bttotb at 30 °C. (c) Adsorption kinetics of nHEX, 3MP, and 22DMB on Al-bttotb at 30 °C. (d) Experimental ternary breakthrough curves of nHEX, 3MP, and 22DMB for Al-bttotb at 30 °C. Reproduced with permission.[38] Copyright 2020, American Chemical Society.

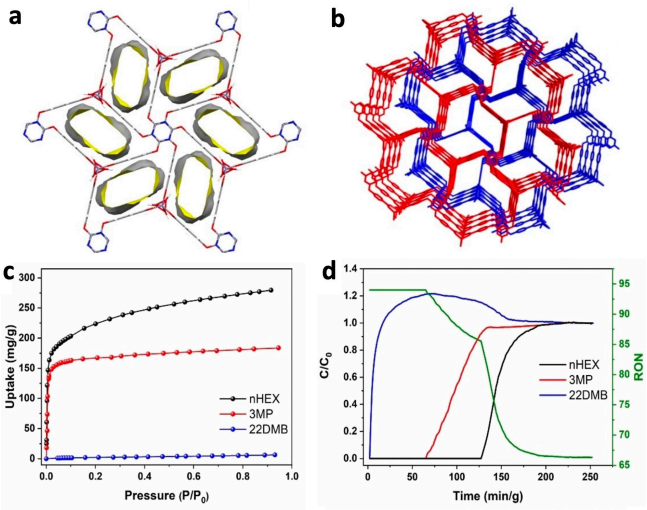

Figure 7. (a–b) Crystal structure of the doubly interpenetrated framework of Zn-tcpt. (c) Adsorption kinetics of nHEX, 3MP, and 22DMB on Zn-tcpt at 303 K. (d) Experimental ternary breakthrough curves of nHEX, 3MP, and 22DMB for Zn-tcpt at 303 K. Reproduced with permission.[42] Copyright 2022, Wiley-VCH.

branched isomer with high octane number elute out from the column without any retention.

4.3. Temperature-Dependent Splitting of C6 Alkane Isomers

Flexible MOFs can change their structures to accommodate the targeted guest molecules, which are additional advantages compared with rigid porous materials for selective separation of alkane isomers.[64] Many flexible MOFs tend to shrink to a smaller pore or even dense and non-porous state after removing the solvent molecules filled in the pores, which responds differently to various adsorbate molecules.[65] Therefore, for MOFs with flexible frameworks, the size and shape of the pores can be precisely controlled by external stimuli (such as adsorbates, pressure, temperature, etc.), thereby giving rise to optimized separation performance for specific gas mixtures.[66] Taking full advantage of this unique structural feature, high-efficiency separation of alkane isomers has been achieved by flexible MOFs.[4]

Structural flexibility often leads to very interesting and unexpected phenomena in a given adsorption process.[8] In 2018, Wang et al. reported the first temperature-dependent separation of alkane isomers based on the flexible microporous MOF, Ca-tcpb (Ca(H_2tcpb), tcpb = 1,2,4,5tetrakis(4-carboxyphenyl)-benzene).[29] Ca-tcpb is a 3D framework constructed by CaO_6 octahedra connected through tcpb ligands. It contains a 1D channels with a cross section of 5.5–6.0 Å (Figure 8a), which is comparable to the kinetic diameter of branched alkanes. Due to its framework flexibility, the adsorption of C6 alkane isomers on Ca-tcpb was highly dependent on the operating temperatures/pressure. Interestingly, it can accommodate both nHEX and 3MP but completely excludes 22DMB at 60 °C, whereas at 120 °C it only adsorbs nHEX (Figure 8b–8c). Thus the temperature-dependent adsorption behavior can be used to facilitate a two-step separation process by molecular exclusion: The branched isomers can be sieved out from the linear isomer at 120 °C, and the di-branched and mono-branched isomers can be subsequently separated at 60 °C (Figure 8d). Column breakthrough experiments confirmed that Ca-tcpb can readily separate a ternary mixture of nHEX/3MP/22DMB into pure individual components through a two-column (set at 120 °C and 60 °C respectively) temperature programming breakthrough system (Figure 8g–8 h). The same behavior was also confirmed by binary breakthrough experiments (Figure 8e–8f). Further powder X-ray diffraction (PXRD) analysis revealed that the temperature-dependent adsorption behavior of Ca-tcpb is a result of its structural flexibility which leads to a change of pore aperture at different temperatures and upon adsorption of different guests (Figure 8i).

In a more recent study, Lin et al. developed a novel flexible MOF, calcium chloranilate (HIAM-203), that exhibits similar temperature-dependent adsorption behavior toward alkane isomers. HIAM-203 features pts topology with chloro-decorated 1D channels (Figure 9a). It demonstrates structural flexibility upon adsorption of various small gases, as well as C6 alkanes with different branching. The compound took up substantial amount of nHEX and 3MP at 30 °C but fully excluded 22DMB, while at 150 °C 3MP was also precluded (Figure 9b–9c). The separation capability of HIAM-203 was confirmed by temperature-programmed two-column breakthrough measurements. The results show that the ternary C6 alkane mixtures were fully separated into individual components according to their branching (Figure 9d).

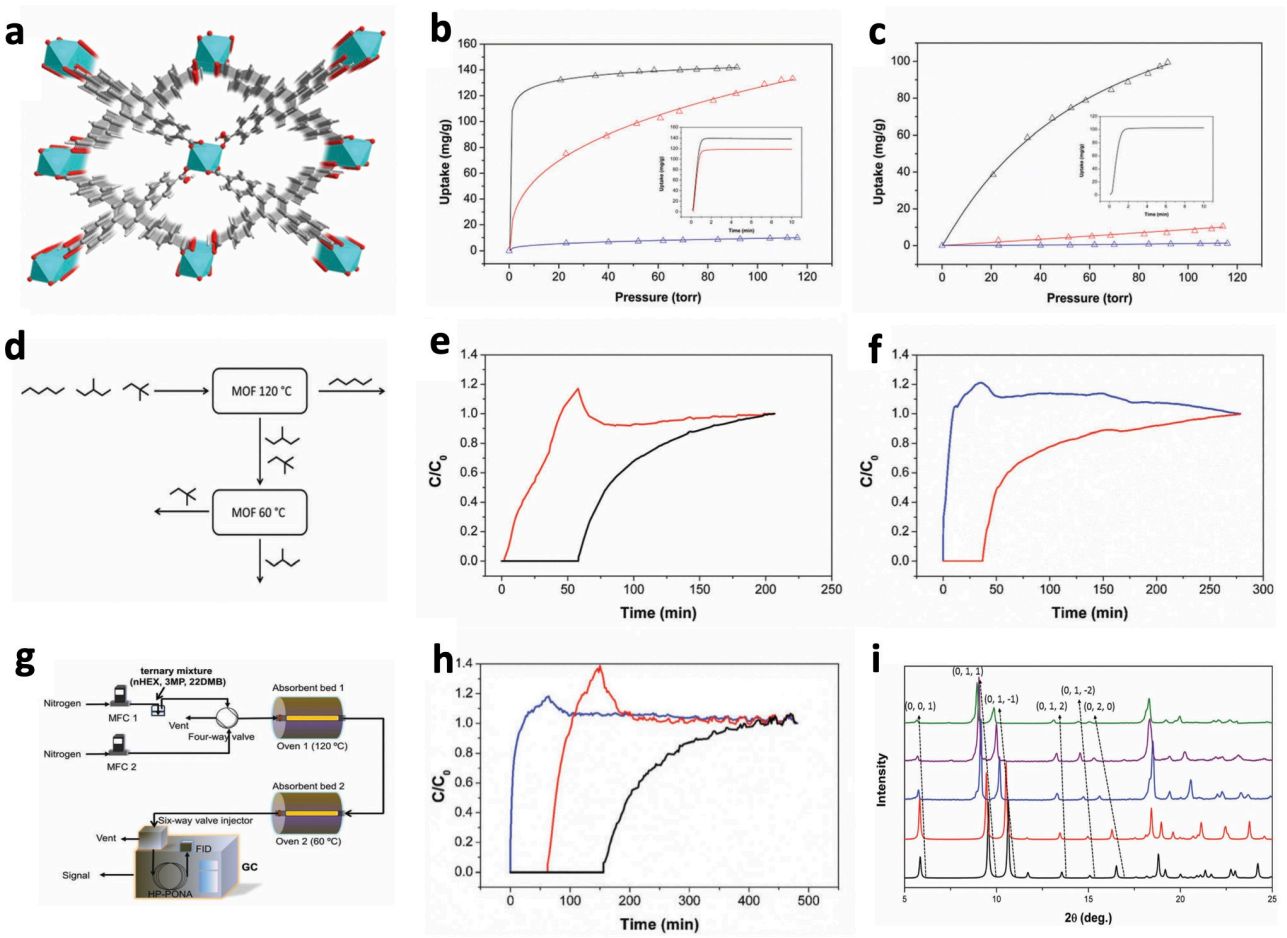

Figure 8. (a) Crystal structure of Ca-tcpb showing the 1D open channels. (b) Adsorption isotherms of nHEX (black), 3MP (red), and 22DMB (blue) at 60 °C. (c) Adsorption isotherms of nHEX (black), 3MP (red), and 22DMB (blue) at 120 °C (inset: the adsorption rates of the corresponding isomers at 100 torrs). (d) Schematic representation of proposed temperature programmed separation of C6 alkane isomers. (e) Experimental binary breakthrough curves of nHEX (black) and 3MP (red) for Ca-tcpb at 120 °C. (f) Experimental binary breakthrough curves of 3MP (red) and 22DMB (blue) for Ca-tcpb at 60 °C. (g) Schematic setup of multicomponent column breakthrough experiments. (h) Experimental ternary breakthrough curves of nHEX (black), 3MP (red), and 22DMB (blue) for Ca-tcpb at 120 °C and 60 °C. (i) PXRD patterns comparison of various forms of Ca-tcpb. From bottom to top: activated (black), as-synthesized (red), loaded with nHEX (blue), loaded with 3MP (purple), and loaded with 22DMB (green). Reproduced with permission.[29] Copyright 2018, Royal Society of Chemistry.

5. Conclusion and Outlook

Adsorptive separation of C6 alkane isomers by porous adsorbents represents a promising solution for producing premium gasoline with upgrading octane number and qualified olefin feed. The great potential of MOF materials with impressive adsorption and separation performance being superior to conventional zeolites has fully expanded beyond the initiative imaginations of scientists and engineers. In this minireview, we have summarized the main advancements in C6 alkane isomers separation by MOFs over the recent years, from early examples to the latest progress in the design of MOFs with desired separation capability. The high-performance separation of C6 alkane isomers by MOFs benefits from the precise engineering of their pore structure as well as the manipulation of the structural flexibility. In particular, the success in addressing the challenging separation of monobranched and dibranched alkanes has been achieved through the fine tailoring of MOF structure.

Although numerous MOFs demonstrating good performance in separating C6 alkane isomers have been achieved, some concerns and challenges remain to be addressed in future research and development prior to industrial implementation. First, the trade-off between adsorption capacity and selectivity must be considered. As summarized in the article most MOFs reported to date exhibit either exceptionally high adsorption capacity or excellent selectivity, but seldomly possess high values for both. More systematic and advanced strategies based on the reticular chemistry need to be established to guide the design of MOFs with optimal pore structure and thus overcome the obstacle properly. Second, high stability and long-term recyclability of MOFs are required in addition to good separation performance. Most reported MOFs still suffer from poor thermal/chemical stability which restricts

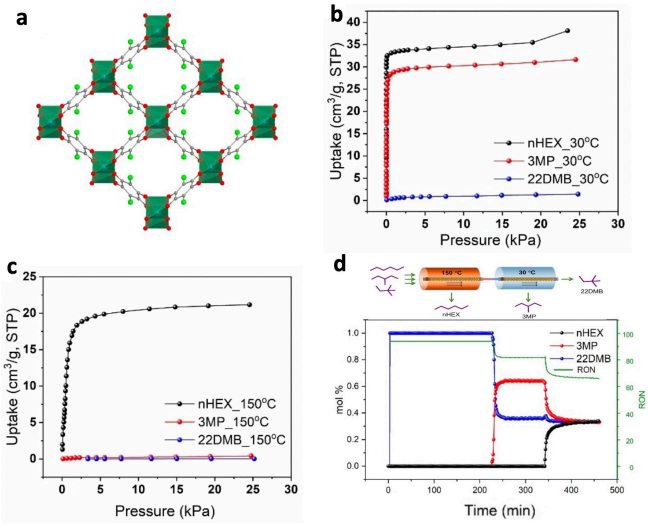

Figure 9. (a) Crystal structure of HIAM-203 with 1D channels. (b) Addsorption isotherms of nHEX, 3MP, and 22DMB on HIAM-203 at 30 °C. (c) Adsorption isotherms of nHEX, 3MP, and 22DMB on HIAM-203 at 150 °C. (d) Schematic representation of temperature programmed separation system and experimental ternary breakthrough curves of nHEX, 3MP, and 22DMB using two columns for HIAM-203 at 150 °C and 30 °C. Reproduced with permission.[45] Copyright 2022, Wiley-VCH.

their implementation in practical applications at the industrial scale. In particular, stability of selected adsorbents should be evaluated under the actual industrial conditions with the presence of possible chemical impurities. The complicated separation conditions in real-world environment (e.g., high moisture, relatively high temperature, and other corrosively acidic impurities) require adsorbents with exceptionally high thermal and chemical stability as well as long-term recyclability. In this regard, various approaches can be implemented to substantially improve the adsorbent resistance toward harsh conditions and environment, including introducing early transition metals or high-valance metals as inorganic building units with strong metal-ligand bonds, high coordination numbers and connectivity. Moreover, industrial separation of naphtha or light naphtha involves much more complicated mixtures than 3–5 alkane components commonly used under the laboratory settings. Thus evaluation of the separation capability of MOF adsorbents for industrially-relevant mixtures, rather than an idealized mixture of simple alkane isomers, is much needed. This has been explored in some pioneering research and preliminary correlations between the naphtha separation performance and MOF structure features have been established. In addition, separation experiments should be performed under industrially desired temperatures and pressure to fully evaluate and assess the feasibility of the MOF candidates for commercial applications. Last but not least, some MOFs reported to date with competitive performance are built on expensive organic ligands and synthesized using complicated procedures, which vastly limit their implementation in practical applications. Therefore, efforts toward low-cost, simple and easily scalable production of MOFs are also very desirable. Despite the existing concerns and challenges, we are optimistic that with continuous efforts in MOF-related research, the adsorptive separation technologies based on MOF adsorbents will eventually be realized in the industrial separation of alkanes.

Acknowledgements

FX and JL would like to thank the U.S. Department of Energy, Office of Science, Office of Basic Energy Sciences (Grant No. DE-SC0019902) for supporting this work. LY and HW acknowledge the financial support from Shenzhen Science and Technology Program (No. RCYX20200714114539243).

Conflict of Interest

The authors declare no conflict of interest.

Keywords: C6 Alkane Isomers · Kinetic Separation · Metal–Organic Frameworks · Selective Size Exclusion · Thermodynamic Separation

[1] R. A. Meyers, *Handbook of Petroleum Refining Processes*, McGraw-Hill Education, New York, **2016**.
[2] A. Aitani, M. N. Akhtar, S. Al-Khattaf, Y. Jin, O. Koseoglo, M. T. Klein, *Energy Fuels* **2019**, *33*, 3828–3843.
[3] G. Valavarasu, B. Sairam, *Pet. Sci. Technol.* **2013**, *31*, 580–595.
[4] H. Wang, Y. Liu, J. Li, *Adv. Mater.* **2020**, *32*, 2002603.
[5] B. Liang, X. He, J. Hou, L. Li, Z. Tang, *Adv. Mater.* **2019**, *31*, 1806090.
[6] Z. Zhang, S. B. Peh, C. Kang, K. Chai, D. Zhao, *EnergyChem* **2021**, *3*, 100057.
[7] H. Wang, D. Luo, E. Velasco, L. Yu, J. Li, *J. Mater. Chem. A* **2021**, *9*, 20874–20896.
[8] W. G. Cui, T. L. Hu, X. H. Bu, *Adv. Mater.* **2020**, *32*, 1806445.
[9] H. Wang, J. Li, *Acc. Chem. Res.* **2019**, *52*, 1968–1978.
[10] A. Luna-Triguero, P. Gomez-Alvarez, S. Calero, *Phys. Chem. Chem. Phys.* **2017**, *19*, 5037–5042.
[11] D. Peralta, G. R. Chaplais, A. L. Simon-Masseron, K. Barthelet, G. D. Pirngruber, *Ind. Eng. Chem. Res.* **2012**, *51*, 4692–4702.
[12] D. I. Kolokolov, S. S. Arzumanov, A. G. Stepanov, H. Jobic, *J. Phys. Chem. C* **2007**, *111*, 4393–4403.
[13] H. Jobic, *J. Mol. Catal. A* **2000**, *158*, 135–142.
[14] S. K. Gade, V. A. Tuan, C. J. Gump, R. D. Noble, J. L. Falconer, *Chem. Commun.* **2001**, 601–602.
[15] R.-B. Lin, S. Xiang, W. Zhou, B. Chen, *Chem* **2020**, *6*, 337–363.
[16] J.-R. Li, R. J. Kuppler, H.-C. Zhou, *Chem. Soc. Rev.* **2009**, *38*, 1477–1504.
[17] H. Furukawa, K. E. Cordova, M. O'Keeffe, O. M. Yaghi, *Science* **2013**, *341*, 1230444.
[18] F. Xie, H. Wang, J. Li, *J. Mater. Chem. A* **2023**, *11*, https://doi.org/10.1039/D2TA09326J.
[19] Z. Bao, J. Wang, Z. Zhang, H. Xing, Q. Yang, Y. Yang, H. Wu, R. Krishna, W. Zhou, B. Chen, *Angew. Chem. Int. Ed.* **2018**, *57*, 16020–16025; *Angew. Chem.* **2018**, *130*, 16252–16257.
[20] A. Cadiau, K. Adil, P. Bhatt, Y. Belmabkhout, M. Eddaoudi, *Science* **2016**, *353*, 137–140.

[21] X. Li, J. Liu, K. Zhou, S. Ullah, H. Wang, J. Zou, T. Thonhauser, J. Li, *J. Am. Chem. Soc.* **2022**, *144*, 21702–21709.
[22] L. Yu, X. Han, H. Wang, S. Ullah, Q. Xia, W. Li, J. Li, I. Da Silva, P. Manuel, S. Rudić, *J. Am. Chem. Soc.* **2021**, *143*, 19300–19305.
[23] F. Xie, H. Wang, J. Li, *Matter* **2022**, *5*, 2516–2518.
[24] X. Cui, K. Chen, H. Xing, Q. Yang, R. Krishna, Z. Bao, H. Wu, W. Zhou, X. Dong, Y. Han, *Science* **2016**, *353*, 141–144.
[25] Y. Jiang, J. Hu, L. Wang, W. Sun, N. Xu, R. Krishna, S. Duttwyler, X. Cui, H. Xing, Y. Zhang, *Angew. Chem. Int. Ed.* **2022**, *61*, e202200947; *Angew. Chem.* **2022**, *134*, e202200947.
[26] Y. Ye, S. Xian, H. Cui, K. Tan, L. Gong, B. Liang, T. Pham, H. Pandey, R. Krishna, P. C. Lan, *J. Am. Chem. Soc.* **2022**, *144*, 1681–1689.
[27] Y. Gu, J. J. Zheng, K. I. Otake, M. Shivanna, S. Sakaki, H. Yoshino, M. Ohba, S. Kawaguchi, Y. Wang, F. Li, *Angew. Chem. Int. Ed.* **2021**, *60*, 11688–11694; *Angew. Chem.* **2021**, *133*, 11794–11800.
[28] Z. Zhang, S. B. Peh, R. Krishna, C. Kang, K. Chai, Y. Wang, D. Shi, D. Zhao, *Angew. Chem. Int. Ed.* **2021**, *60*, 17198–17204; *Angew. Chem.* **2021**, *133*, 17335–17341.
[29] H. Wang, X. Dong, E. Velasco, D. H. Olson, Y. Han, J. Li, *Energy Environ. Sci.* **2018**, *11*, 1226–1231.
[30] H. Wang, X. Dong, J. Lin, S. J. Teat, S. Jensen, J. Cure, E. V. Alexandrov, Q. Xia, K. Tan, Q. Wang, *Nat. Commun.* **2018**, *9*, 1745.
[31] Z. R. Herm, B. M. Wiers, J. A. Mason, J. M. van Baten, M. R. Hudson, P. Zajdel, C. M. Brown, N. Masciocchi, R. Krishna, J. R. Long, *Science* **2013**, *340*, 960–964.
[32] X. Li, Y. Lin, L. Yu, J. Zou, H. Wang, *Inorg. Chem.* **2022**, *61*, 13229–13233.
[33] Q. Yu, L. Guo, D. Lai, Z. Zhang, Q. Yang, Y. Yang, Q. Ren, Z. Bao, *Sep. Purif. Technol.* **2021**, *268*, 118646.
[34] R. Banerjee, A. Phan, B. Wang, C. Knobler, H. Furukawa, M. O'Keeffe, O. M. Yaghi, *Science* **2008**, *319*, 939–943.
[35] L. Chen, S. Yuan, J.-F. Qian, W. Fan, M.-Y. He, Q. Chen, Z.-H. Zhang, *Ind. Eng. Chem. Res.* **2016**, *55*, 10751–10757.
[36] P. A. Mendes, P. Horcajada, S. Rives, H. Ren, A. E. Rodrigues, T. Devic, E. Magnier, P. Trens, H. Jobic, J. Ollivier, *Adv. Funct. Mater.* **2014**, *24*, 7666–7673.
[37] R. Chen, F. Zhou, B. Sheng, Z. Zhang, Q. Yang, Y. Yang, Q. Ren, Z. Bao, *ACS Sustainable Chem. Eng.* **2022**, *10*, 11330–11337.
[38] L. Yu, X. Dong, Q. Gong, S. R. Acharya, Y. Lin, H. Wang, Y. Han, T. Thonhauser, J. Li, *J. Am. Chem. Soc.* **2020**, *142*, 6925–6929.
[39] H. Wang, X. Dong, J. Ding, K. Wang, L. Yu, S. Zhang, Y. Han, Q. Gong, A. Ma, J. Li, *Chem. Eur. J.* **2021**, *27*, 11795–11798.
[40] L. Yu, S. Ullah, K. Zhou, Q. Xia, H. Wang, S. Tu, J. Huang, H.-L. Xia, X.-Y. Liu, T. Thonhauser, *J. Am. Chem. Soc.* **2022**, *144*, 3766–3770.
[41] Z. Zhang, S. B. Peh, C. Kang, K. Yu, D. Zhao, *Angew. Chem. Int. Ed.* **2022**, *61*, e202211808; *Angew. Chem.* **2022**, *134*, e202211808.
[42] L. Yu, S. Ullah, H. Wang, Q. Xia, T. Thonhauser, J. Li, *Angew. Chem. Int. Ed.* **2022**, *61*, e202211359; *Angew. Chem.* **2022**, *134*, e202211359.
[43] Q. Chen, S. Xian, X. Dong, Y. Liu, H. Wang, D. H. Olson, L. J. Williams, Y. Han, X. H. Bu, J. Li, *Angew. Chem. Int. Ed.* **2021**, *60*, 10593–10597; *Angew. Chem.* **2021**, *133*, 10687–10691.
[44] E. Velasco, S. Xian, H. Wang, S. J. Teat, D. H. Olson, K. Tan, S. Ullah, T. M. Osborn Popp, A. D. Bernstein, K. A. Oyekan, *ACS Appl. Mater. Interfaces* **2021**, *13*, 51997–52005.
[45] Y. Lin, L. Yu, S. Ullah, X. Li, H. Wang, Q. Xia, T. Thonhauser, J. Li, *Angew. Chem. Int. Ed.* **2022**, *61*, e202214060; *Angew. Chem.* **2022**, *134*, e202214060.
[46] A. T. Balaban, *Pure Appl. Chem.* **1983**, *55*, 199–206.
[47] B. Chen, C. Liang, J. Yang, D. S. Contreras, Y. L. Clancy, E. B. Lobkovsky, O. M. Yaghi, S. Dai, *Angew. Chem. Int. Ed.* **2006**, *45*, 1390–1393; *Angew. Chem.* **2006**, *118*, 1418–1421.
[48] H. Wang, X. Dong, V. Colombo, Q. Wang, Y. Liu, W. Liu, X. L. Wang, X. Y. Huang, D. M. Proserpio, A. Sironi, *Adv. Mater.* **2018**, *30*, 1805088.
[49] H. Belarbi, L. Boudjema, C. Shepherd, N. Ramsahye, G. Toquer, J.-S. Chang, P. Trens, *Colloids Surf. A* **2017**, *520*, 46–52.
[50] A. Henrique, A. E. Rodrigues, J. A. Silva, *Ind. Eng. Chem. Res.* **2019**, *58*, 378–394.
[51] D. Lv, H. Wang, Y. Chen, F. Xu, R. Shi, Z. Liu, X. Wang, S. J. Teat, Q. Xia, Z. Li, *ACS Appl. Mater. Interfaces* **2018**, *10*, 6031–6038.
[52] Y. Ling, Z.-X. Chen, F.-P. Zhai, Y.-M. Zhou, L.-H. Weng, D.-Y. Zhao, *Chem. Commun.* **2011**, *47*, 7197–7199.
[53] W. Fan, X. Zhang, Z. Kang, X. Liu, D. Sun, *Coord. Chem. Rev.* **2021**, *443*, 213968.
[54] D. Britt, H. Furukawa, B. Wang, T. G. Glover, O. M. Yaghi, *Proc. Natl. Acad. Sci. USA* **2009**, *106*, 20637–20640.
[55] Y. Wang, C. Hao, W. Fan, M. Fu, X. Wang, Z. Wang, L. Zhu, Y. Li, X. Lu, F. Dai, *Angew. Chem. Int. Ed.* **2021**, *60*, 11350–11358; *Angew. Chem.* **2021**, *133*, 11451–11459.
[56] J. Lee, C. Y. Chuah, J. Kim, Y. Kim, N. Ko, Y. Seo, K. Kim, T. H. Bae, E. Lee, *Angew. Chem. Int. Ed.* **2018**, *57*, 7869–7873; *Angew. Chem.* **2018**, *130*, 7995–7999.
[57] Y. Wang, D. Zhao, *Cryst. Growth Des.* **2017**, *17*, 2291–2308.
[58] P. A. Mendes, A. E. Rodrigues, P. Horcajada, C. Serre, J. A. Silva, *Microporous Mesoporous Mater.* **2014**, *194*, 146–156.
[59] K. S. Park, Z. Ni, A. P. Côté, J. Y. Choi, R. Huang, F. J. Uribe-Romo, H. K. Chae, M. O'Keeffe, O. M. Yaghi, *Proc. Natl. Acad. Sci. USA* **2006**, *103*, 10186–10191.
[60] N. Chang, Z.-Y. Gu, X.-P. Yan, *J. Am. Chem. Soc.* **2010**, *132*, 13645–13647.
[61] T. Devic, P. Horcajada, C. Serre, F. Salles, G. Maurin, B. Moulin, D. Heurtaux, G. Clet, A. Vimont, J.-M. Greneche, *J. Am. Chem. Soc.* **2010**, *132*, 1127–1136.
[62] H.-C. Zhou, J. R. Long, O. M. Yaghi, *Chem. Rev.* **2012**, *112*, 673–674.
[63] Q. Gong, L. Yu, J. Ding, S. Zhang, Y. Bo, K. Chi, H. Wang, Q. Xia, S. He, J. Li, *Sep. Purif. Technol.* **2022**, *294*, 121219.
[64] S. Horike, S. Shimomura, S. Kitagawa, *Nat. Chem.* **2009**, *1*, 695–704.
[65] N. Nijem, P. Thissen, Y. Yao, R. C. Longo, K. Roodenko, H. Wu, Y. Zhao, K. Cho, J. Li, D. C. Langreth, *J. Am. Chem. Soc.* **2011**, *133*, 12849–12857.
[66] H. Wang, M. Warren, J. Jagiello, S. Jensen, S. K. Ghose, K. Tan, L. Yu, T. J. Emge, T. Thonhauser, J. Li, *J. Am. Chem. Soc.* **2020**, *142*, 20088–20097.

Manuscript received: January 17, 2023
Accepted manuscript online: February 16, 2023
Version of record online: ■■, ■■

Minireviews

Alkane Separation

F. Xie, L. Yu, H. Wang,*
J. Li* **e202300722**

Metal-Organic Frameworks for C6 Alkane Separation

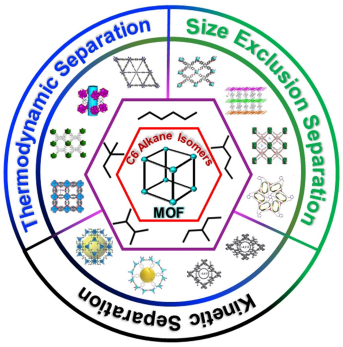

This minireview summarizes the recent advancement in developing MOFs as energy-efficient adsorbents for the separation of C6 alkane isomers based on different separation mechanisms. Particular emphasis is made on the design and tailoring of their structures and pore properties to achieve optimal separation performance. Existing challenges and possible solutions, as well as future directions of this important research field is also discussed.